

INFLUENCE OF Nb₂O₅ AND B₂O₃ ON THE PHOTOCATALYTIC AND ANTIBACTERIAL ACTIVITY OF SOL-GEL DERIVED TiO₂ NANOPOWDERS

Albena Bachvarova-Nedelcheva¹, Reni Iordanova¹, Nelly Georgieva²,
Veronica Nemska², Tsvetelina Foteva², Angelina Stoyanova³

¹Institute of General and Inorganic Chemistry
Bulgarian Academy of Sciences
Acad. G. Bonchev Str. bl. 11, 1113 Sofia, Bulgaria

²Department of Biotechnology
University of Chemical Technology and Metallurgy
8 Kliment Ohridski Blvd, 1797 Sofia, Bulgaria

³Department of Chemistry and Biochemistry
Faculty of Pharmacy, Medical University-Pleven
1 Kliment Ohridski Str., 5800 Pleven, Bulgaria
E-mail: albenadb@svr.igic.bas.bg

Received 09 July 2023

Accepted 20 December 2023

DOI: 10.59957/jctm.v59.i2.2024.12

ABSTRACT

TiO₂ based powders containing B₂O₃ and Nb₂O₅ were obtained through an aqueous sol-gel method. The as-prepared gels were step wisely heated in the temperature range 200°C - 500°C and subsequently characterized by XRD, IR and UV-Vis analysis. The TiO₂ (anatase) is the single crystalline phase which has been detected up to 500°C. Photocatalytic tests showed that the investigated samples possess photocatalytic activity toward Malachite green organic dye and TiO₂/Nb₂O₅ exhibited higher photocatalytic activity than TiO₂/B₂O₃ sample. The compositions exhibited good antimicrobial activity against *E. coli* NBIMCC K12 407 and *Bacillus subtilis* NBIMCC 3562.

Keywords: sol-gel, powders, antibacterial properties, photocatalytic properties.

INTRODUCTION

The titania and TiO₂ based compounds are subjects of special interest and they are intensively studied mainly due to their good photocatalytic and antibacterial properties [1, 2]. A semiconductor with photocatalytic activities TiO₂ has great potential as a self-cleaning and self-disinfecting material. Moreover, due to its high photoreactivity it has been broadly used for killing different groups of microorganisms including bacteria, fungi and viruses [3 - 4]. It was found that TiO₂ NPs decompose organic compounds by the formation and constant release of hydroxyl radicals and superoxide ions when exposed to non-lethal ultraviolet (UV) light [5], which can be used against bacteria and other organic substances [2].

Various methods for synthesis like hydrothermal route, sol-gel route and wet impregnation have been

studied for doped TiO₂ nanopowders. Among them, the sol-gel process is the most widely used approach consisting of two steps: hydrolysis of a titanium salt and a further condensation reaction. It was found that this method leads to obtaining of greatest homogeneous distribution of the dopant in the host matrix and high surface area of as-prepared TiO₂ particles [6]. It is well known that the sol - gel synthesis allows the possibility of synthesizing new materials with designed properties. TiO₂ shows relatively high reactivity and chemical stability under ultraviolet light ($\lambda < 387\text{nm}$), whose energy exceeds the band gap of 3.3 eV in the anatase crystalline phase [7].

Our group has a great deal of experience preparing TiO₂ composite powders by sol-gel technique. With this method, we successfully produced many binary, ternary, and multicomponent composites with improved photocatalytic and antibacterial qualities [8 - 12].

This work is an extension of our earlier studies on the sol-gel synthesis of powdered TiO₂ nanocomposite. Since the emphasis is now on compositions with enhanced photocatalytic and antibacterial capabilities, the search for novel not yet studied compositions has been expanded. The originality of the current work is highlighted by the lack of published data on binary TiO₂/B₂O₃ and TiO₂/Nb₂O₅ sol-gel derived powders and studies of their antibacterial and photocatalytic applications.

The present study is focused on the sol - gel synthesis and characterization of two binary TiO₂ containing gels modified with B₂O₃ and Nb₂O₅. An attempt to compare the influence of both oxides on the photocatalytic and antibacterial activity of the as prepared nanopowders was made.

EXPERIMENTAL

Samples preparation

Based on our previous study on the gel formation in different binary TiO₂ - M_nO_m systems [13, 14], two compositions containing 80 mol % TiO₂ were selected - 80TiO₂.20B₂O₃ and 80TiO₂.20Nb₂O₅, denoted as TB and TN, respectively. Both samples were subjected to detailed investigations. Ti(IV) n-butoxide (Fluka AG), H₃BO₃ (Merck) niobium(V) ethoxide (C₁₀H₂₅NbO₅) as precursors dissolved in ethylene glycol (C₂H₆O₂) (99% Aldrich) were used. The dissolving in ethylene glycol was performed by vigorous magnetic stirring. Transparent gels were obtained and followed by heat treatment at 200°C in air in order to hydrolyze unreacted -OR groups as well as to decrease their content. Aiming to verify the phase and structural transformations, the gels were subjected to further stepwise heating from 200°C to 500°C. The calcination of the samples was performed for 2 hours exposure time in air, until obtaining powder. The calcination temperature was selected on the basis of our previous investigations [10, 13]. The pH during the experiments was measured at 7.5 - 8.0. The photocatalytic properties of both powdered samples were compared with those of a commercial TiO₂ (Fluka).

Samples characterization

Powder XRD patterns were registered at room temperature using a Bruker D8 Advance X-ray powder

diffractometer, Cu Kα radiation ($k = 1.54056 \text{ \AA}$) with a LynxEye solid position sensitive detector and X - ray tube operated at 40 kV and 40 mA. X-ray diffraction patterns were recorded in the range of 5.3 - 80° 2 θ with a step of 0.02° 2 θ. The optical absorption spectra of the powdered samples in the wavelength range 200 nm - 700 nm were recorded by a UV - VIS diffused reflectance Spectrophotometer "Evolution 300" using a magnesium oxide reflectance standard as a baseline. The band gap energies (E_g) of the samples were calculated by the Planck's equation (1):

$$A_g = \frac{h.c}{\lambda} = \frac{1240}{\lambda} \quad (1)$$

where E_g is the band gap energy (eV), h is the Planck's constant, c is the light velocity (m.s⁻¹), and λ is the wavelength (nm). The specific surface areas (BETs) were determined by low-temperature (77.4 K) nitrogen adsorption in NOVA 1200e surface area and pore analyzer at relative pressures $p/p_0 = 0.1 - 0.3$ using BET equation.

Photocatalytic activity experiments

Photocatalytic decomposition capabilities of the synthesized samples were evaluated under UV - light illumination by taking Malachite green (MG) as model dye pollutant. In the photocatalytic test, 100 mg of each sample was suspended in 150 mL MG aqueous solution. For all experiments, the concentration of MG dye was 5 ppm. Before irradiation, the suspensions were magnetically stirred and maintained for 30 min in the dark to attain the absorption-desorption equilibrium between the dye molecules and the photocatalyst surface. Irradiation with UV - light was provided by a black light blue lamp (Sylvania BLB 50 Hz 8W T5) with the major fraction of irradiation occurring at 365 nm. The lamp was fixed above the solution surface and the distance between the solution and the UV source was constant, 10 cm. Each MG/catalyst suspension has been exposed to UV - light with vigorous stirring. The zero timing was the moment of the UV lamp switching on. Sampling was performed at regular time during reaction. An aliquot (3 mL) of the suspensions was extracted from the photoreacted mixture and centrifuged to remove the catalyst particles. The extent of photodegradation efficiency of the studied samples can be represented by the degradation percentage of MG dye, which was calculated by obtaining the relationship

between C/C_0 and illumination time (min), where C and C_0 are the concentrations of MG dye at time t and time zero, respectively. The MG concentration changes (C/C_0) are directly proportional to absorbance changes (A/A_0) during photodecomposition. So the percentage of degradation of MG dye ($D\%$) was calculated using the following equation (2):

$$D\% = 1 - \frac{A_t}{A_0} \times 100 \quad (2)$$

where A_0 is absorbance of the dye at zero time and A_t is the absorbance at a time t during degradation process.

Antimicrobial test

Two reference strains of bacteria were used to examine the evaluated materials' antibacterial capabilities - *Escherichia coli* NBIMCC K12 407 and *Bacillus subtilis* NBIMCC 3562. They were provided by the National Bank for Industrial Microorganisms and Cell Cultures (NBIMCC, Bulgaria) and cultivated in Luria-Bertani (LB, HiMedia, Mumbai, India) broth and Nutrient broth (NB, HiMedia, Mumbai, India) on a shaker-incubator ES - 20/60 (Biosan, Riga, Latvia, 120 rpm) at 37°C/30°C, respectively for 24 h. The process of

evaluating the antibacterial activity of materials consists of calculating the cell reduction of strains after exposure to them. Each flask contained 10 mg of each ingredient, 100 μ L of the strain solution ($OD_{610\text{ nm}} = 1.9$), and 100 mL of liquid broth in order to achieve the main goal. Only the controls flasks had additional materials added to them. Petri dishes with 50 μ L of each flask's culture broth was added to sterile agar, which was then incubated in an incubator (Binder, Germany) at 37°C/30°C for 24 h. Based on the number of colonies that have grown, the percentage of cell decrease was computed [15 - 17]. Every test was performed three times, and the mean values were displayed in the final results.

RESULTS AND DISCUSSION

Phase transformations

The purity, crystallinity and phase formation of investigated samples (TB and TN) calcined at different temperatures (200°C - 500°C) were analyzed by XRD. The XRD patterns of the powdered samples are shown in Fig. 1. At low temperature (200°C) both samples are amorphous. The increasing of temperatures showed that TN samples preserves the amorphous state up to

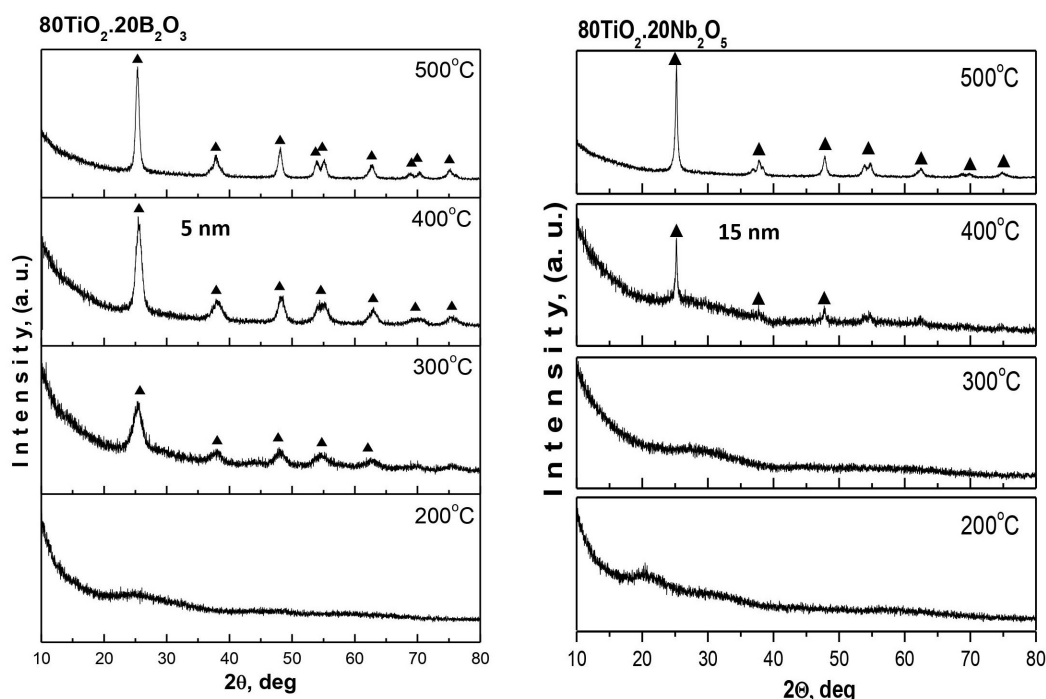


Fig. 1. XRD patterns of investigated samples heat treated at different temperatures: (■) Te, (▲) TiO₂- anatase, (*) TiO₂- rutile, (●) TiTe₃O₈.

400°C while for sample TB first TiO₂ (anatase, JCPDS 78 - 2486) crystals appeared already at 300°C. The TiO₂ (anatase) is the single crystalline phase which has been detected up to 500°C. The XRD pattern of TB sample at 400°C is showing a broad peak typical of nanosized crystallites. The average crystallite size of the particles, calculated from the broadening of the diffraction line using Sherrer's equation is about 5 nm (sample TB) and 15 nm (sample TN). The specific surface area (SSA) results using Brunauer - Emmett - Teller (BET) nitrogen adsorption experiments showed that SSA for the TiO₂/Nb₂O₃ sample was higher and had a value of 70 m² g⁻¹, while the other TiO₂/Nb₂O₃ sample exhibited lower SSA value - 35 m²/g. The obtained XRD data are very similar to those obtained by other teams [18, 19].

UV-Vis DRS characterization

The UV – visible analysis is considered a powerful tool for exploring the optical features of nanocomposite powders. Numerous factors influence the absorbance, such as surface, impurity centers, oxygen deficiency, and bandgap [20]. The optical absorption spectra of investigated gels TB and TN were compared to those of pure TiO₂ obtained by Ti(IV) butoxide gel (Fig. 2). The absorption edge and optical band gap values of the samples are summarized in Table 1. The UV - Vis spectra exhibit two maxima 230 - 260 nm and 300 - 325 nm which could be assigned to the isolated TiO₄ and TiO₆ units, respectively [21]. As shown on the figure, for TBT gel, the intensity of UV peaks in the spectra at 230 nm and that near 325 nm are comparable which is an indication of the commensurate amount of TiO₄ and TiO₆ polyhedra in the gel network. The same was observed for the spectra of TB gel, while for TN sample the peak at 305 nm is slightly stronger than the other at 230 nm, which is an indication of more completed hydrolysis - condensation reactions. The UV - Vis spectra were also used to determine the optical band gap (E_{opt}) of investigated sample (Table 1). The obtained results suggest that Nb₂O₅ did not extend the absorbance of TiO₂ to the visible light. There are some contradictions in the literature concerning the influence of Nb₂O₅ on the band gap. Some authors [22] found that there is no difference in the band gap of pure TiO₂ and Nb doped TiO₂. However, Yang et al. reported a reduced band gap for Nb - doped TiO₂ porous microspheres [23]. This behavior could be attributed to the particle morphology

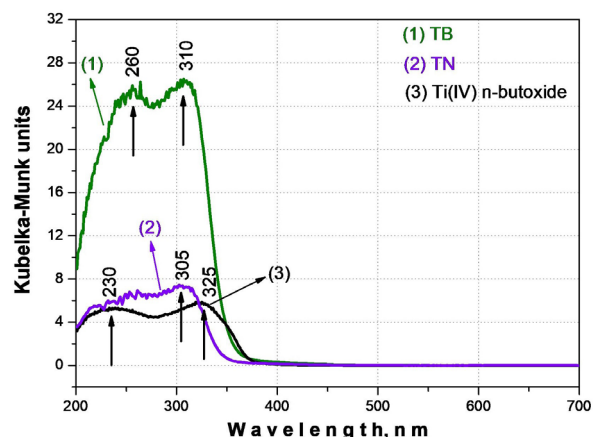


Fig. 2. UV-Vis spectra of investigated gels compared with Ti(IV) butoxide.

Table 1. Observed cut-off and calculated bandgap values of selected samples.

-	Gel composition	Cut-off, nm	Eg, eV
1.	Ti(IV) butoxide	375	3.31
2.	80TiO ₂ .20Nb ₂ O ₃	348	3.56
3.	80TiO ₂ .20B ₂ O ₃	353	3.51

and/or distribution of Nb₂O₅ on TiO₂. Looking back to our results, it is seen that both samples showed similar values for Eg (TN - 3.56 eV, TB - 3.51 eV) which is slightly higher than that of pure TiO₂ (3.31 eV), (Table 1). Obviously, further experiment has to be performed in order to clarify this phenomenon.

Photocatalytic activity

The photocatalytic action of pure and modified TiO₂ powders heated at 500°C for 1 h was tested for degradation of MG dye water solution illuminated with UV light. The MG dye has been selected as a model pollutant for our investigation on account of its extensive discharge as an industrial effluent coupled with its hazardous impacts on human health and marine life. For comparison, the MG dye degradation was also followed in the presence of commercial TiO₂ (Fluka). Fig. 3(a, b) depicts the percentage removal of MG dye as a function of irradiation time. As can be seen from the figure, the best photocatalytic activity showed the commercial TiO₂ (Fluka) with 100 % decoloration efficiency in 60 min irradiation. After 90

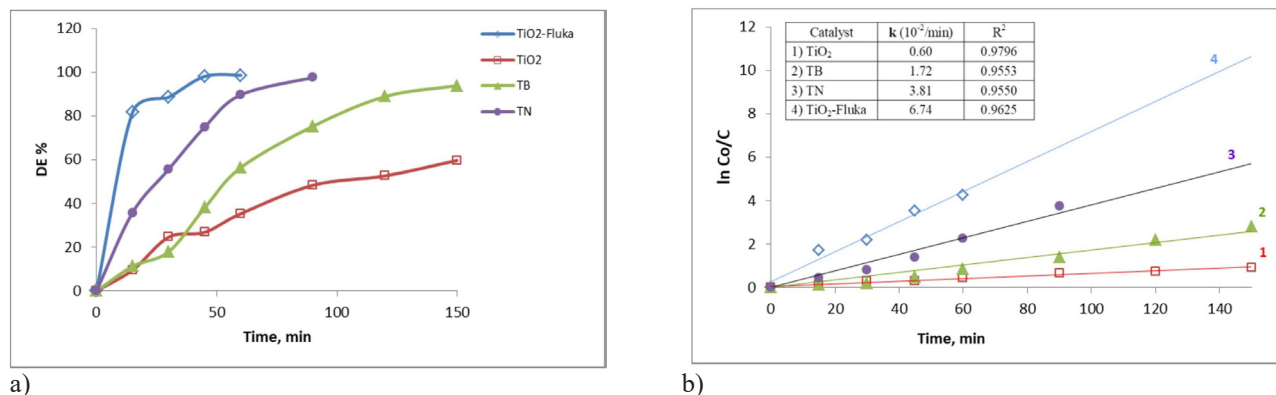


Fig. 3. (a) Photodegradation efficiency of TiO₂, TB, TN and TiO₂ - Fluka samples in decoloration of MG under UV irradiation; (b) Photocatalytic reaction kinetics of MG decoloration by investigated samples.

min of irradiation the percentage removal of MG dye was nearly 100 % using TN and 75 % using TB. Thus, the removal efficiency of TN was better than that of TB and similar to the commercial product under the same conditions (Fig. 3(a)). Obviously, the modified TB and TN samples exhibited better photoactivity than the synthesized pure TiO₂.

These results were confirmed by the application of pseudo - first order kinetic model as expressed by the equation $\ln C_0/C_t = kt$, which is generally used for photocatalytic degradation processes [24], where C_0 and C_t are the concentrations of dye at time 0 and t, respectively, and k is the pseudo - first order constant (Fig. 3(b)). A good correlation to the pseudo - first order kinetics ($R^2 > 0.955$) was found from these results. The rate constants of the samples are 0.0060, 0.0172 and 0.0381 min⁻¹ for the synthesized pure TiO₂, TB and TN, respectively.

Bearing in mind the fact that the photocatalytic activity of doped TiO₂ depends on many factors (synthesis method, dopant concentration, light source, particle size, surface area, etc.) it could be summarized that the higher SSA (70 m² g⁻¹) of the TN sample could be the reason for its better photocatalytic activity. Obviously, at our experimental conditions, the presence of boron oxide was less beneficial than introducing of niobium oxide to the photoactivity under UV irradiation.

Antibacterial tests

The investigated TN and TB samples heat-treated at 200°C and 400°C have been tested for antibacterial activity against *E. coli* NBIMCC K12 407 and *Bacillus subtilis* NBIMCC 3562. The testing has been performed by monitoring the cell reduction of cultivated

microorganisms in the presence of investigated materials for 24 hours in a liquid medium, Tables 2(a, b). Both tested powdered materials showed good antibacterial properties against *E. coli* NBIMCC K12 407. It was observed the tendency that the heat - treated materials at 200°C revealed higher antibacterial activity towards the Gram-negative strain in comparison to the same materials treated at 400°C, Table 2(a).

The experiments concerning the influence of materials on the cell growth of *Bacillus subtilis* NBIMCC 3562 demonstrated that only the TN sample treated at 200°C showed 30.2 % cell reduction in comparison to the 9.3 % reduction by the TN sample treated at 400°C (Table 2(b)). The Gram - positive strain was more sensitive to the heat-treated at 400°C TB sample which exhibited 52.5 % cell reduction. The heated at 200°C TB powders showed 35 % cell reduction. Obviously, the TiO₂ modified with B₂O₃ possess better antibacterial ability toward both bacterial strains. We suggest that these observations could be explained by the XRD results (Fig. 1). According to these findings the presence of amorphous part is preserved at 200°C and in sample TN even at 400°C. Therefore, observed antibacterial activity could be explained by the synergetic effect of anatase and presence of amorphous phase in the samples at both temperatures. Our investigations well correspond to these obtained by Dědkova et al. which found that the presence of amorphous state in the Ce doped TiO₂ materials is one of the reasons for their good antibacterial activity [25]. Thus, it could be concluded that the amorphous state also contributes to the good antibacterial properties of the obtained composite powders.

Table 2a. Antibacterial test results for tested materials against *E. coli* NBIMCC K12 407 after 24h incubation. Data are expressed as means \pm SD (n =3).

Samples	<i>E. coli</i> NBIMCC K12 407	
	CFU mL ⁻¹	Cell reduction, %
Control	5 \times 10 ⁹	-
80TiO ₂ /20B ₂ O ₃ (200°) (TB)	3.1 \times 10 ⁹	38%
80TiO ₂ /20B ₂ O ₃ (400°) (TB)	3.5 \times 10 ⁹	30%
Control	1.35 \times 10 ⁸	-
80TiO ₂ /20Nb ₂ O ₅ (200°) (TN)	1.15 \times 10 ⁸	14.8%
80TiO ₂ /20Nb ₂ O ₅ (400°) (TN)	1.25 \times 10 ⁸	7.4%

Table 2b. Antibacterial test results for tested materials against *B. subtilis* NBIMCC 3562 after 24h incubation. Data are expressed as means \pm SD (n =3).

Samples	<i>Bacillus subtilis</i> NBIMCC 3562	
	CFU mL ⁻¹	Cell reduction, %
Control	4 \times 10 ⁸	-
80TiO ₂ /20B ₂ O ₃ (200°) (TB)	2.6 \times 10 ⁸	35%
80TiO ₂ /20B ₂ O ₃ (400°) (TB)	1.9 \times 10 ⁸	52.5%
Control	4.3 \times 10 ⁷	-
80TiO ₂ /20Nb ₂ O ₅ (200°) (TN)	3.0 \times 10 ⁷	30.2%
80TiO ₂ /20Nb ₂ O ₅ (400°) (TN)	3.9 \times 10 ⁷	9.3%

CONCLUSIONS

Two gels 80TiO₂/20B₂O₃ and 80TiO₂/20Nb₂O₅ were obtained by aqueous sol - gel method and subjected to detailed investigations. It was established by XRD and IR analysis that the niobium oxide preserved the organic constituents up to 300°C and the organic - inorganic amorphous phase completely transformed into inorganic one above 400°C. The TiO₂ (anatase) is the single crystalline phase which has been detected up to 500°C. Two maxima about 230 - 260 nm and 305 - 325 nm related to the isolated TiO₄ units and condensed TiO₆ groups were registered by UV - Vis spectroscopy. The modified with boron and niobium oxide samples exhibited better removal efficiency than the synthesized pure TiO₂. The photocatalytic test reveals that the addition of niobium oxide stimulates the degradation of the MG dye and its photocatalytic activity is better than those of TiO₂/B₂O₃. Both investigated compositions showed good antimicrobial

activity against *E. coli* NBIMCC K12 407 and *Bacillus subtilis* NBIMCC 3562. As a result, further research is required to develop new powdered compositions aiming to improve their applications.

Acknowledgements

The authors are thankful for the financial support by the project Project CoE "National Center of Mechatronics and Clean Technologies" (BG05M2OP001-1.001-0008).

REFERENCES

1. O. Carp, C. Z. Huisman, A. Reller, Progress in Solid State Chemistry, 32, 2004, 33-177.
2. A. Fujishima, T. Rao, D. Tryk, J. Photochem. Photobiol. C: Photochem. Rev., 1, 2000, 1-21.
3. X. Chen, S.S. Mao, Titanium dioxide nanomaterials: synthesis, properties, modifications and applications, Chem. Rev., 107, 7, 2007, 2891-2959.

4. P.C. Maness, S. Smolinski, D.M. Blake, Z. Huang, E.J. Wolfrum, W.A. Jacoby, Bactericidal activity of photocatalytic TiO₂ reaction: toward an understanding of its killing mechanism, *Appl. Environ. Microbiol.*, 65, 1999, 4094-4098.
5. M.S.A. Shah, M. Nag, T. Kalagara, S. Singh, S.V. Manorama, Silver on PEG-PU-TiO₂ polymer nanocomposite films; an excellent system for antibacterial applications, *Chem. Materials*, 20, 2008, 2455-2460.
6. L. Chen, K. Rahme, J.D. Holmes, M.A. Morris, N.K.H. Slater, Non-solvolytic synthesis of aqueous soluble TiO₂ nanoparticles and real-time dynamic measurements of the nanoparticle formation, *Nanoscale Res. Lett.*, 7, 2012, 297-397.
7. A. Zaleska, Doped-TiO₂: Review, *Recent Patents on Engineering*, 2, 2008, 157-164.
8. A. Stoyanova, A. Bachvarova-Nedelcheva, R. Iordanova, N. Ivanova, H. Hitkova, M. Sredkova, Synthesis, photocatalytic and antibacterial properties of nanosized ZnTiO₃ powders obtained by different sol-gel methods. *Digest J. Nanomater. Biostr.*, 7, 2, 2012, 777-784.
9. A. Shalaby, A. Bachvarova-Nedelcheva, R. Iordanova, Y. Dimitriev, A. Stoyanova, H. Hitkova, N. Ivanova, Sol-gel synthesis and properties of nanocomposites in the Ag/TiO₂/ZnO system, *J. Optoelect. Adv. Mater.*, 17, 1-2, 2015, 248-256.
10. A. Bachvarova-Nedelcheva, R. Iordanova, A. Stoyanova, N. Georgieva, Ts. Angelova, Sol-gel synthesis of Se and Te containing TiO₂ nanocomposites with photocatalytic and antibacterial properties. *J. Optoelect. Adv. Mater.*, 18, 1-2, 2016, 5-9.
11. R. Gegova, A. Bachvarova-Nedelcheva, R. Iordanova, Y. Dimitriev, Synthesis and crystallization of gels in the TiO₂-TeO₂-ZnO system, *Bulg. Chem. Commun.*, 47, 1, 2015, 378-386.
12. A. Stoyanova, H. Hitkova, A. Bachvarova Nedelcheva, R. Iordanova, N. Ivanova, M. Sredkova, Synthesis and antibacterial activity of TiO₂/ZnO nanocomposites prepared via nonhydrolytic route. *J. Chem. Techn. Metall.*, 48, 2, 2013, 154-161.
13. R. Iordanova, R. Gegova, A. Bachvarova-Nedelcheva, Y. Dimitriev, Sol-gel synthesis of composites in the ternary TiO₂-TeO₂-B₂O₃ system, *Phys. Chem. Glasses: Eur. J. Glass Sci. Technol. B*, 56, 4, 2015, 128-138.
14. A. Bachvarova-Nedelcheva, R. Iordanova, R. Gegova, Y. Dimitriev, Crystallization of gels in the binary TiO₂-M_nO_m (M_nO_m = TeO₂, SeO₂, B₂O₃, ZnO) systems, *Bulg. Chem. Commun.*, 49, special issue A, 2017, 110-118.
15. A. Bachvarova-Nedelcheva, R. Iordanova, A. Stoyanova, N. Georgieva, T. Angelova, Sol-gel synthesis of Se and Te containing TiO₂ nanocomposites with photocatalytic and antibacterial properties. *J. Optoelect. Adv. Mater.*, 18, 2016, 5-9.
16. Ts. Angelova, N. Rangelova, N. Georgieva. Antifungal properties of SiO₂/hydroxypropyl cellulose hybrid materials doped with zinc ions against *Candida albicans* 74, *Food Science and Applied Biotechnology*, 1, 2, 2018, 104-107.
17. Ts. Foteva, N. Georgieva, Antimicrobial properties of silica/hydroxypropylcellulose hybrids doped with copper ions, *Journal of Chemical Technology and Metallurgy*, 57, 5, 2022, 930-936.
18. A.L. da Silva, D.N.F. Muche, S. Dey, D. Hotza, Ricardo H.R. Castro, Photocatalytic Nb₂O₅-doped TiO₂ nanoparticles for glazed ceramic tiles, *Ceram. Intern.*, 42, 2016, 5113-5122.
19. Catia Liane Ücker, Fabio Riemke, Vitor Goetzke, Mario Lúcio Moreira, Cristiane Wienke Raubach, Elson Longo, Sergio Cava, Facile preparation of Nb₂O₅/TiO₂ heterostructures for photocatalytic application, *Chem. Phys. Impact*, 4, 2022, 100079-100086.
20. A. Bachvarova-Nedelcheva, R. Iordanova, A. Naydenov, A. Stoyanova, N. Georgieva, V. Nemska, Ts. Foteva, Sol-gel obtaining of TiO₂/TeO₂ nanopowders with biocidal and environmental applications, *Catalysts*, 13, 2023, 257-274.
21. V. Barlier, V. Bounor-Legare, G. Boiteux, J. Davenas, Hydrolysis–condensation reactions of titanium alkoxides in thin films: A study of the steric hindrance effect by X-ray photoelectron spectroscopy, *Appl. Surf. Sci.*, 254, 2008, 5408-5412.
22. A.L. Castro, M.R. Nunes, M.D. Carvalho, L.P. Ferreira, J.-C. Jumas, F.M. Costa, M.H. Florencio, Doped titanium dioxide nanocrystalline powders with high photocatalytic activity, *J. Solid State Chem.*, 182, 2009, 1838-1845.
23. J. Yang, X. Zhang, C. Wang, P. Sun, L. Wang, B. Xia, Solar photocatalytic activities of porous Nb-doped TiO₂ microspheres prepared by ultrasonic

- spray pyrolysis, *Solid State Sci.*, 14, 2012, 139-144.
24. K. Kumar, K. Porkodi, F. Rocha, Langmuir-Hinshelwood kinetics-A theoretical study, *Catal. Comm.*, 9, 2008, 82-84.
25. K. Dědková, L. Matějová, K. Matějová, P. Peikertová, K. Mamulova Kutlaková, J. Kukutschová, *Nanocon-2013*, 16-18.10, 2013, Brno, Czech Republic.